

Au-Mo-Fe-Ni/CeO₂(Gd₂O₃) As Potential Fuel Electrodes For Internal CO₂ Reforming of CH₄ in Single SOFCs

E. Ioannidou*, S. Neophytides, and D. K. Niakolas

Foundation for Research and Technology, Institute of Chemical Engineering Sciences (FORTH/ICEHT), Stadiou Str., 26504, Platani, Patras, Greece

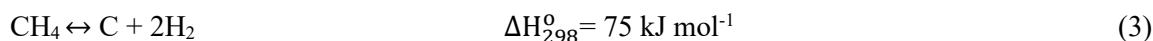
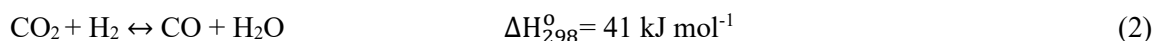
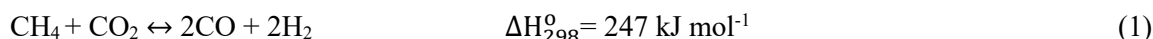
**eiouannidou@iceht.forth.gr*

Keywords: single SOFCs; Internal CO₂ reforming of CH₄; Au-Mo-Fe-Ni/GDC electrodes; biogas

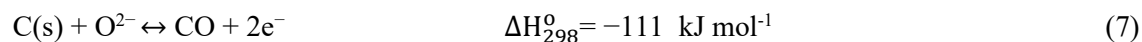
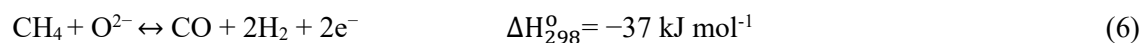
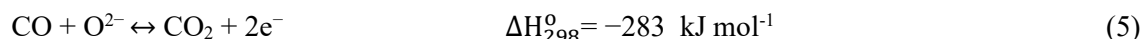
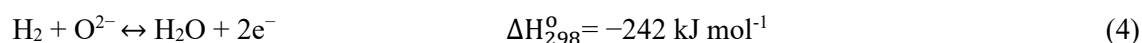
1. Introduction

Recycling biogas to produce syngas (H₂ + CO) through Dry Reforming of Methane (DRM) has currently attracted resurgent interest. Biogas consists mainly of CH₄ (50-70%) and CO₂ (25-50%) and is widely produced by anaerobic fermentation of biomass [1]. DRM provides a feasible solution to eliminate greenhouse gases via production of useful chemicals and hydrocarbons.

Considering the DRM energy applications the produced syngas can be used as a fuel in high temperature solid oxide fuel cells (SOFCs) for electricity production or biogas can be directly fueled in the cell without the need of an external reformer (Internal Dry Reforming of Methane, IDRM), which simplifies the SOFC system and reduces the cost [2,3]. When biogas is directly fed to the SOFC fuel electrode at temperatures 750-900 °C, various catalytic and electrocatalytic reactions may take place simultaneously on the electrode (Eq. 1-7) [4,5].



The CO₂ reforming of methane (DRM) (Eq. 1) is a strongly endothermic process and therefore high temperatures (typically >750 °C) are required to achieve high H₂ and CO yields [6]. Moreover, the catalytic Reverse Water Gas Shift (RWGS) reaction (Eq. 2) may run in parallel, resulting in the consumption of valuable H₂ and a decrease in H₂/CO ratio to values lower than unity [7]. In addition, carbon deposition on the electrocatalyst surface due to CH₄ decomposition (Eq. 3) may also occur resulting in progressive electrocatalyst deactivation [8,9]. The CH₄ decomposition (Eq. 3) is favoured at high temperatures (> 600 °C), whereas at temperatures below 650 °C carbon deposits are mainly produced by Boudouard reaction (2CO → C + CO₂) [7-9]. The H₂, CO and C produced, as well as the CH₄ supplied can be electrochemically oxidized by oxygen ions according to Eq. 4-7.



Ni-based ceramic-metal composites with Ytria Stabilized Zirconia (YSZ) and Gadolinia Doped Ceria (GDC or CeO₂(Gd₂O₃)) are widely used as electrocatalysts in SOFCs because of their activity and inexpensiveness. According to the literature, Ni/GDC fuel electrodes show higher electrocatalytic activity for CH₄ reforming, resistance to carbon deposition, and tolerance levels for H₂S compared to Ni/YSZ electrodes [10,11]. Authors attributed this behaviour to the capacity of CeO₂ to store and release oxygen, which favours the CH₄ oxidation and mitigates the carbon deposition [1,12]. The carbon tolerance and anti-sintering tendency of nickel can be enhanced further, by dispersing trace amounts of transition noble (Rh, Pt, Pd, Ru, Au) or non-noble (Co, Cu, Mo, Fe) metal elements [3,13].

In this study the catalytic and electro-catalytic performance, as well as the coking resistance of unmodified and modified Ni/CeO₂(Gd₂O₃) with 3 wt.% Au-0.4 wt.% Mo and 3 wt.% Au-0.5 wt.% Fe electrocatalysts were studied as half and full electrolyte supported cells under internal CO₂ reforming

of CH₄ in single SOFCs, at 750-900 °C. The aim was to elucidate their activity towards the consumption of CH₄, CO₂, the production of H₂, H₂O, CO and the production of carbon, as a function of temperature and the applied current density under a biogas fuel mixture of CH₄/CO₂=1. Additionally, the cells comprising the electrocatalysts as fuel electrodes, 8 mol% Y₂O₃ stabilized ZrO₂ (8YSZ) as electrolyte and La_{0.6}Sr_{0.4}Co_{0.8}Fe_{0.2}O_{3-δ} (LSCoF) as oxygen electrode were characterized using I-V measurements and Electrochemical Impedance Spectra (EIS) analysis in order to investigate the evolution of the ohmic and polarization resistance values as a reflection of current.

2. Results

The catalytic-kinetic measurements were performed with gas flows in the range of 150-300 cm³/min, where the reactor was operating under differential conditions with reactants' conversions between 5-20%. In the above gas flow range the reaction rates were found to remain practically constant, which corresponds to the absence of mass transfer limitations. Figure 1 presents the Arrhenius plots for the consumption rates of CH₄ and CO₂, under differential conditions, and the derived apparent activation energies ($E_{a,app}$) for each electrocatalyst. It is observed that the modified electrodes were less active for CH₄ and CO₂ consumption with relatively high $E_{a,app}$ values, compared to unmodified Ni/GDC. According to the literature [14], non-carbon forming CH₄ activation is the rate-determining step at high temperatures for both DRM and decomposition reactions. Furthermore, it is known that CH₄ is activated on metal surface sites (e.g. Ni), whereas CO₂ is mainly activated on support sites (e.g. GDC) in the vicinity of dispersed metal particles or/and on the metallic sites [7]. In the presented study the calculated $E_{a,app}$ for Ni/GDC is 63 kJ/mol for CH₄ activation, which coincides with the $E_{a,app}$ for CH₄ dissociation on Ni (1 1 0) and Ni (1 1 1) [15].

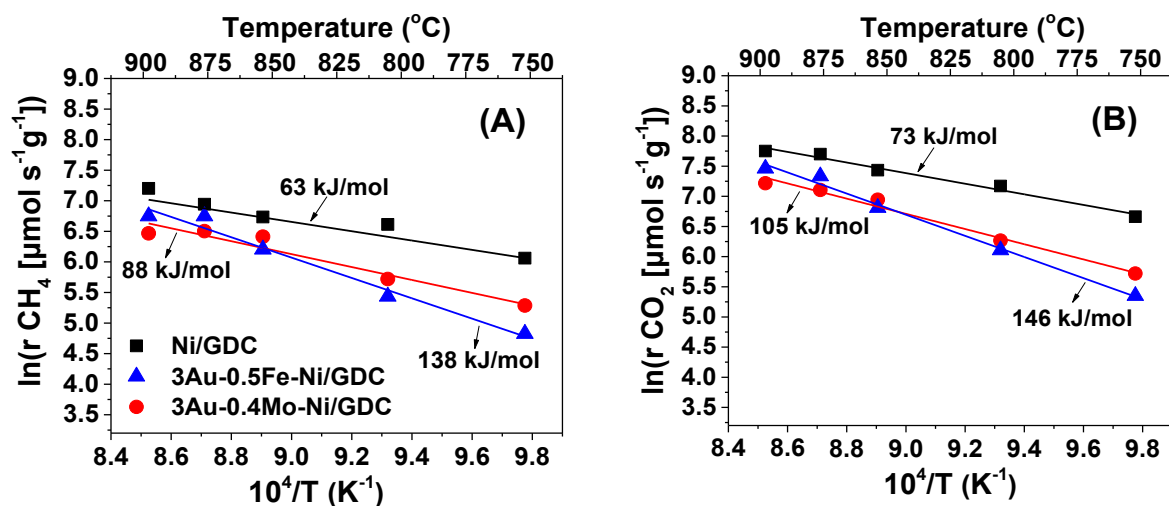


Figure 1. Arrhenius plots of the inherent consumption of (A) CH₄ and (B) CO₂ rates as a function of temperature (750-900 °C). The corresponding apparent activation energies ($E_{a,app}$, kJ/mol) are embedded. Open circuit potential and differential conditions under the mixture of 50 vol.% CH₄–50 vol.% CO₂. F_{total} is varied, 150-300 cm³/min. Electrode mass ~6 mg/cm².

Furthermore, according to the catalytic measurements, the modified 3Au-0.5Fe-Ni/GDC and 3Au-0.4Mo-Ni/GDC electrodes were less active for H₂ and CO production, but at the same time were less prone to carbon formation, compared to Ni/GDC.

Figure 2 shows the characteristic i-V curves of the SOFCs comprising Ni/GDC, 3Au-0.5Fe-Ni/GDC and 3Au-0.4Mo-Ni/GDC as anodes, under a mixture of CH₄/CO₂=1, without dilution in a carrier gas, at 900 and 850 °C. Specifically, the cell with 3Au-0.5Fe-Ni/GDC exhibited the best performance, at both temperatures, since it provided in a wider range of current density at the same applied potential, compared to the other cells. In addition, the cell with 3Au-0.4Mo-Ni/GDC performed better than that with Ni/GDC, but worse than that with 3Au-0.5Fe-Ni/GDC. Another interesting observation is the effect of temperature on the performance, confirming that the highest temperature promoted faster kinetics, which is reflected on the higher performance of the cells and the lower slopes in the i-V curves.

It should be remarked that the cell with Ni/GDC exhibited the worst electrocatalytic performance for the IDR process, compared to the cells with the modified electrodes, despite its higher DRM catalytic activity. This may be related to the different structural properties of Au-Mo and Au-Fe modified Ni/GDC electrodes. For this purpose, detailed physicochemical measurements are currently in progress, focusing on the changes of bulk and surface properties of the electrodes.

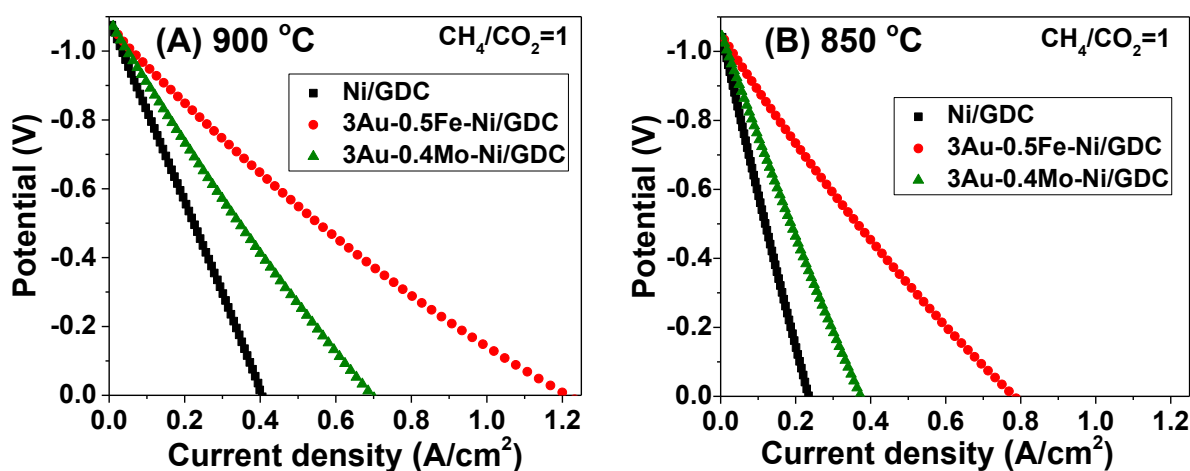


Figure 2. Polarization (i-V) curves at (A) 900 °C and (B) 850 °C for ESCs comprising Ni/GDC, 3Au-0.5Fe-Ni/GDC and 3Au-0.4Mo-Ni/GDC as fuel electrodes. IDR conditions under a mixture of 50 vol.% CH₄-50 vol.% CO₂. $F_{\text{total, in}} = 50 \text{ cm}^3/\text{min}$.

Acknowledgments

This research has been co-financed by the European Union and Greek national funds through the operational program ‘Regional Excellence’ and the operational program ‘Competitiveness, Entrepreneurship and Innovation’, under the call “RESEARCH-CREATE-INNOVATE” (Project code: T2EAK-00955).

References

1. M.J. Escudero, C.A. Maffiotte and J.L. Serrano, *J. Power Sources*, **481**, 229048 (2021).
2. S. Souentie, M. Athanasiou, D.K. Niakolas, A. Katsaounis, S.G. Neophytides and C.G. Vayenas, *J. Catal.*, **306**, 116-128 (2013).
3. Ch. Neofytidis, V. Dracopoulos, S.G. Neophytides and D.K. Niakolas, *Catal. Tod.*, **310**, 157-165 (2018).
4. M.J. Escudero and J.L. Serrano, *Int. J. Hydrogen En.*, **44** (36) 20616-20631 (2019).
5. M. Chlipała, P. Błaszczaka, S.F. Wang and B. Bochentyna, *Int. J. Hydrogen En.*, **44** (26) 13864-13874 (2019).
6. N.A.K. Aramouni, J.G. Touma, B.A. Tarbousha, J. Zeaitera and M.N. Ahmad, *Renewable and Sust. Energy Rev.* **82**, 2570-2585 (2018).
7. I.V. Yentekakis, P. Panagiotopoulou and G. Artemakis, *Applied Cat. B.: Environ.*, **296**, 120210 (2021).
8. D. Pakhare and J. Spivey, *Chem. Soc. Rev.*, **43**, 7813-7837 (2014).
9. M.K. Nikoo and N.A.S. Amin, *Fuel Process. Technol.*, **92**, 678-691 (2011).
10. M.A. Abdelkareem, W.H. Tanveer and E.T. Sayed, *Renew. Sustain. Ener. Rev.*, **101**, 361-375 (2019).
11. W. Wang, C. Su, Y. Wu, R. Ran and Z. Shao, *Chem. Rev.*, **113**, 8104-8151 (2013).
12. N. Mahato, A. Banerjee, A. Gupta, S. Omar and K. Balania, *Prog. Mater. Sci.*, **72**, 141-337 (2015).
13. D.K. Niakolas, J.P. Ouweltjes, G. Rietveld, V. Dracopoulos and S.G. Neophytides, *Int. J. Hydrogen En.*, **35**, 7898-1904 (2010).
14. A. Kambolis, H. Matralis, A. Trovarelli and C. Papadopoulou, *Appl. Catal. A Gen.*, **377** (1-2), 16-26 (2010).
15. I. Luisetto, S. Tuti, C. Romano, M. Boaro and E. Di Bartolomeo, *J. CO2 Util.*, **30**, 63-78 (2019).